CORA Cork Open Research Archive
Cartlann Taighde Oscailte Chorcaí

Title	Nonhydrostatic Pollard-like internal geophysical waves
Authors	Kluczek, Mateusz
Publication date	2019-05-01
Original Citation	Kluczek, M. (2019) 'Nonhydrostatic Pollard-like internal geophysical waves'. Discrete and Continuous Dynamical Systems, 39, pp. 5171-5183. doi: 10.3934/dcds.2019210
Type of publication	Article (peer-reviewed)
Link to publisher's version	http://aimsciences.org//article/doi/10.3934/dcds.2019210 - 10.3934/dcds.2019210
Rights	© 2019 American Institute of Mathematical Sciences. This is a pre-copy-editing, author-produced PDF of an article accepted for publication in Discrete and Continuous Dynamical Systems - Series A following peer review. The definitive publisher-authenticated version is available online at: http://aimsciences.org//article/doi/10.3934/dcds.2019210
Download date	2026-11-03 02:53:27
Item downloaded from	https://hdl.handle.net/10468/8066

UCC
University College Cork, Ireland
Coláiste na hOllscoile Corcaigh

Nonhydrostatic Pollard-like internal geophysical waves

Mateusz Kluczek
School of Mathematical Sciences
University College Cork, Cork, Ireland
m.kluczek@umail.ucc.ie

Abstract

We present a new exact and explicit Pollard-like solution describing internal water waves representing the oscillation of the thermocline in a nonhydrostatic model. The derived solution is a modification of Pollard's surface wave solution in order to describe internal water waves at general latitudes. The novelty of this model consists in the embodiment of transitional layers beneath the thermocline. We present a Lagrangian analysis of the nonlinear internal water waves and we show the existence of two modes of the wave motion.

Keywords: Exact and explicit solution; geophysical, internal water waves;

2010 Mathematics Subject Classification: 76B15, 86A05, 74G05

1 Introduction

The aim of this paper is to construct a new exact solution of the geophysical fluid dynamics governing equations at a fixed latitude which prescribes an internal wave motion representing the oscillation of the thermocline. The important aspect of this solution is that it includes the effects of the Earth's rotation. The author presented an exact internal water wave solution in [35] for a model assuming that the water is still beneath the thermocline. Consequently, we develop a more realistic scenario, which requires the imposition of transitional layers. In this new model the transition from the oscillation of the thermocline to the still deep water is realised by means of a current flowing beneath the thermocline. Therefore, the flow characteristics are quite different to those presented in [35] and result in a new additional second slow wave mode being a nonlinear phenomenon.

Quite recently the classical Gerstner solution [44] is of great interest to the mathematical society. It results in number of papers deriving solutions for various geophysical waves, e.g. equatorially-trapped waves [5–7, 22, 25, 26], waves in the presence of underlying depth-invariant currents [9, 13, 20, 21, 23, 33, 34, 41], and a solution for trapped waves at an arbitrary latitude [16] with an instability analysis of Gerstner-like solutions in [8, 29]. The mathematical importance of those solutions is presented in [24, 29, 31]; cf. [2] for a discussion of the oceanographical relevance of those solutions. Moreover, new exact and explicit three-dimensional solutions of the nonlinear governing equations capturing strong depth variations of the flow are given in [11–13, 30, 31].

Although, it is remarkable that Gerstner's solution can describe such unique and complex flows, the solution is more suitable for flows close to the equator. Pollard modified Gerstner's solution and derived a new extended solution applicable at higher latitudes to rotating flows [38]. In this new solution the planetary vorticity affects the waves and causes a slight cross-wave tilt to the wave orbital motion [14, 35,38]. The particles paths are still described as closed circles in the fixed reference framework [14, 38]. However, the circles are now in the plane slightly tilted to the local vertical, whereas in Gerstner's solution the plane is genuinely vertical [3]. Consequently, the wave-current interactions in Pollard's solution for surface waves are described in [14] by including in the exact solution an underlying depth-invariant current interpreted as the mean flow velocity. Moreover, an instability of this solution is available in [27,28] and the solution has been proven to be globally dynamically possible [40].

Following Pollard's work on the surface wave solution we construct a new internal water wave solution of the nonlinear governing equations in the nonhydrostatic model. We derive a dispersion relation for the nonhydrostatic model and by a suitable non-dimensional change of variables we transform it to a polynomial equation of degree six. The degree of the resulting polynomial is dependent on the complexity of the model, therefore introducing additional layers beneath the thermocline we increase the degree of the polynomial — the polynomial derived for a model with one layer beneath the thermocline is of order four, which is the case presented in [35]. An analysis of the polynomial identifies four roots, which are equivalent to two modes of the internal water wave in the dimensional terms; one is a standard internal gravity wave modified slightly by the rotation of Earth and one is a slow mode describing almost inertial circles made by a particle of water. We hope that our study serves as a window to a genuine understanding of complex geophysical flows across Earth [10].

2 Governing equation

Geophysical fluid dynamics refers to natural flows, which have appropriate physical scaling such that the effects of the Earth's rotation play an appreciable role [15]. The rotation of the fluid due to the planetary rotation and the stratification are two significant physical features of the geophysical flows [17]. In order to accommodate the Earth's rotation, the flow pattern we investigate is described in a rotating frame with the origin at a point on the Earth's surface. The stratification of the fluid is represented by a consideration of a thermocline, which is explained in more detail in section 3. The Earth is taken to be a sphere of a radius $R = 6371$ km, rotating with a constant rotational speed $\Omega = 7.29 \times 10^{-5}$ rad s^{-1} round the polar axis towards the east. The Cartesian coordinates (x, y, z) represent the directions of the longitude, latitude and local vertical, where (u, v, w) is the velocity field. The governing equations for the geophysical ocean waves, where the viscous effects are neglected, are given by the Euler's equations [15, 37]

$$\begin{cases} u_t + uu_x + vu_y + wu_z + 2\Omega w\cos\phi - 2\Omega v\sin\phi = -\frac{1}{\rho}P_x, \\ v_t + uv_x + vv_y + wv_z + 2\Omega u\sin\phi = -\frac{1}{\rho}P_y, \\ w_t + uw_x + vw_y + ww_z - 2\Omega u\cos\phi = -\frac{1}{\rho}P_z - g. \end{cases}$$

In the aforementioned equations t is time, ϕ represents the latitude, $g = 9.81$ m s^{-2} is the constant gravitational acceleration at the Earth's surface, P is the pressure and ρ is the density of water. In order to complete the governing equations the density is taken as a piecewise constant function resulting in the continuity equation

$$u_x + v_y + w_z = 0, \tag{1}$$

for each region of constant density. We investigate the internal water waves in a relatively narrow ocean strip less then a few degrees of latitude wide. Therefore, the f-plane approximation of the governing equation is used [15, 19, 43]. The Euler equations in the f-plane are expressed by taking the Coriolis parameters

$$f = 2\Omega\sin\phi, \qquad \hat{f} = 2\Omega\cos\phi,$$

as constants [15] at a fixed latitude. Thus, the equations reduce to

$$\begin{cases} u_t + uu_x + vu_y + wu_z + \hat{f}w - fv = -\frac{1}{\rho}P_x, \\ v_t + uv_x + vv_y + wv_z + fu = -\frac{1}{\rho}P_y, \\ w_t + uw_x + vw_y + ww_z - \hat{f}u = -\frac{1}{\rho}P_z - g. \end{cases} \tag{2}$$

For further description of the model we introduce the quotient $\tilde{f} = f/\hat{f} = \tan\phi$, which is a constant at a fixed latitude.

3 Description of the nonhydrostatic model

In this section we give a short description of the layered model used in the study of the exact and explicit solution derived here. We extend the hydrostatic model described in [35] by way of a series of transitional layers which represents a transition from the region where the internal water waves propagate to the motionless abyssal deep-water region (cf. Figure 1).

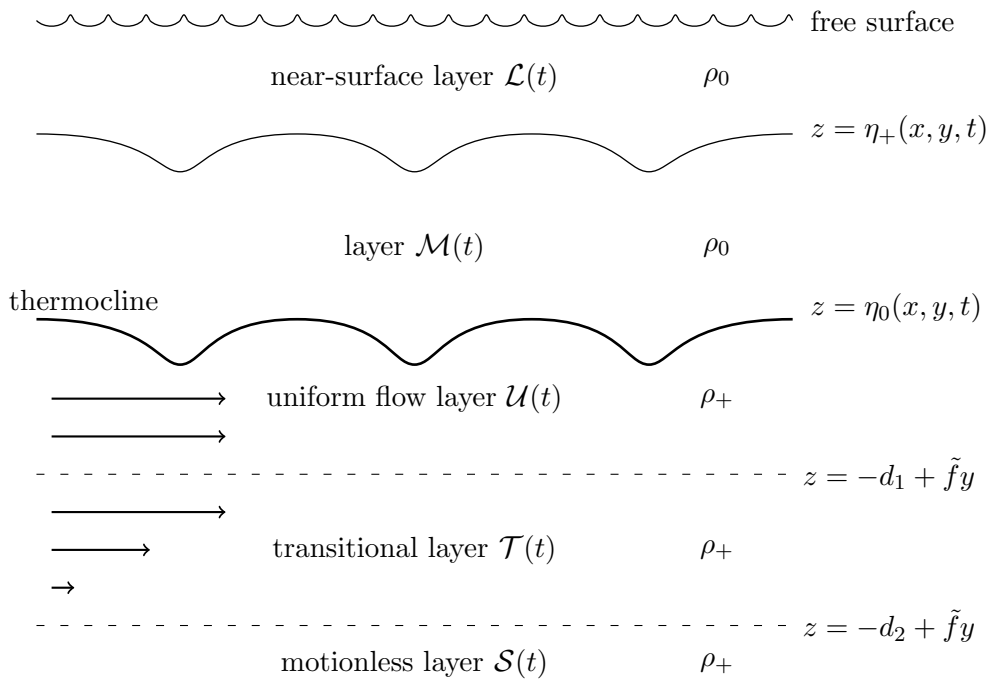


Figure 1: The nonhydrostatic model and its flow regions for fixed y and ϕ. The thermocline separates two layers of ocean water with different but constant densities $\rho_+ > \rho_0$ in a stable stratification [15, 18, 43]. The thermocline is described by a trochoid propagating with the phase speed c. The transitional layer $\mathcal{T}(t)$ provide a transition from the wave motion region to the motionless abyssal deep-water region of the ocean. The schematic is presented for fixed $\tilde{f} = f/\hat{f} = \tan\phi$.

In a stable stratification two horizontal layers of oceanic water of constant but different densities $\rho_+ > \rho_0$ are separated by a thermocline [15,18,43]. The oscillating thermocline is in the shape of a trochoid propagating with the phase speed c, which is quite different to the setting of surface waves, which are described by an inverted trochoid [3, 4, 14]. The geophysical internal water waves represents the oscillation of the thermocline and propagate above the thermocline. The thermocline is a phenomenon occurring predominantly at latitudes in the range $\phi \sim 75^\circ$ N–75° S. In the subpolar regions of Earth ($\phi > 75^\circ$ N or S) the temperature of water is constant [18] and therefore, the conditions prevailing there do not support the ex-

istence of the thermocline. In the flow discussed here the amplitude of the internal water waves decreases with the height above the thermocline in the exponential rate and at the hight of half a wave-length it is less than 4% of its value at the thermocline. We present the internal water waves in the nonhydrostatic model. The model is described as follows (cf. Figure 1). The thermocline oscillates and induces the fluid motion above the thermocline in the layer $\mathcal{M}(t)$. Below the thermocline we introduce the uniform flow layer $\mathcal{U}(t)$ accommodating a uniform horizontal current in the direction of the wave propagation. Beneath $\mathcal{U}(t)$ there is the transitional layer $\mathcal{T}(t)$ where the horizontal velocity of the fluid decreases linearly with the depth. Finally, we have the motionless abyssal deep-water layer $\mathcal{S}(t)$ where the water is still. We distinguish two regions in the fresh and less dense oceanic water above the thermocline, because the flow induced by the oscillating thermocline dies out exponentially fast as one ascends in the fluid. We separate the layer $\mathcal{M}(t)$, where the geophysical internal water wave propagates, and the near-surface layer $\mathcal{L}(t)$ where the geophysical effect is neglected. The motion in the layer $\mathcal{L}(t)$ is a small perturbation of the free surface caused primarily by the wind. The nonhydrostatic model was used previously in [7,33] to describe internal water waves represented by solutions symmetric about the equator in the β-plane approximation. The aim of this paper is to generalise [7] for an arbitrary latitude in the f-plane.

4 Main result

The solution for the nonlinear internal water waves is constructed by building up from the motionless layer and it has to be developed for each layer of the fluid separately. It is a delicate matter since the normal components of the velocity and pressure have to be continuous across each interface. We seek for a solution to (2) keeping in mind that when we work above the thermocline we denote the density of less dense water as ρ_0 and when we work below the thermocline the density of more dense and colder water is referred as ρ_+. To complete the governing equations we introduce the kinematic condition at each interface in the nonhydrostatic model

$$w = \frac{\partial \eta_i}{\partial t} + u\frac{\partial \eta_i}{\partial x} + v\frac{\partial \eta_i}{\partial y} \text{ on } z = \eta_i(x, y, t) \text{ for } i = 0, 1, 2. \tag{3}$$

preventing mixing particles of water between layers. The solution is designed as follows. First, we find a suitable velocity field satisfying the appropriate kinematic conditions in each layer and next, a pressure continuous at the interfaces satisfying the governing equations.

The motionless layer $\mathcal{S}(t)$

For the motionless layer we define the upper boundary of the layer

$$z = \eta_2(x, y, t) = -d_2 + \tilde{f}y,$$

for some fixed depth $d_2 > 0$ and $\tilde{f} = f/\hat{f} = \tan\phi$, where the assumption of the infinite depth of water is taken into consideration. The velocity field of the still water is

$$u = v = w = 0 \qquad z \leq -d_2 + \tilde{f}y.$$

It implies the hydrostatic pressure

$$P(x, y, z, t) = P_0 - \rho_+ g z \qquad z \leq -d_2 + \tilde{f}y,$$

where P_0 is an arbitrary constant.

The transitional layer $\mathcal{T}(t)$

Above the interface $\eta_2(x, y, t) = -d_2 + \tilde{f}y$ we distinguish the transitional layer with the upper boundary

$$z = \eta_1(x, y, t) = -d_1 + \tilde{f}y,$$

where $d_2 > d_1 > 0$. The horizontal velocity of water's particles increases linearly in this layer. Taking into account appropriate boundary conditions

$$u = 0 \text{ on } z = -d_2 + \tilde{f}y$$
$$u = c \text{ on } z = -d_1 + \tilde{f}y$$

we obtain the horizontal component of the velocity field

$$u(y, z) = \frac{c}{d_2 - d_1}(z + d_2 - \tilde{f}y).$$

with the meridional and vertical velocities

$$v = w = 0.$$

Substituting the above into the governing equations we get the pressure function for the transitional layer

$$P(x, y, z, t) = \frac{1}{2}\frac{c}{d_2 - d_1}\rho_+ \hat{f}\left(z + d_2 - \tilde{f}y\right)^2 - \rho_+ g z + P_0.$$

We note that the upper and lower interface of the transitional layer is tilted at an angle ϕ to the local meridional axis. It is a manifestation of the effects of the Earth's rotation at higher latitudes.

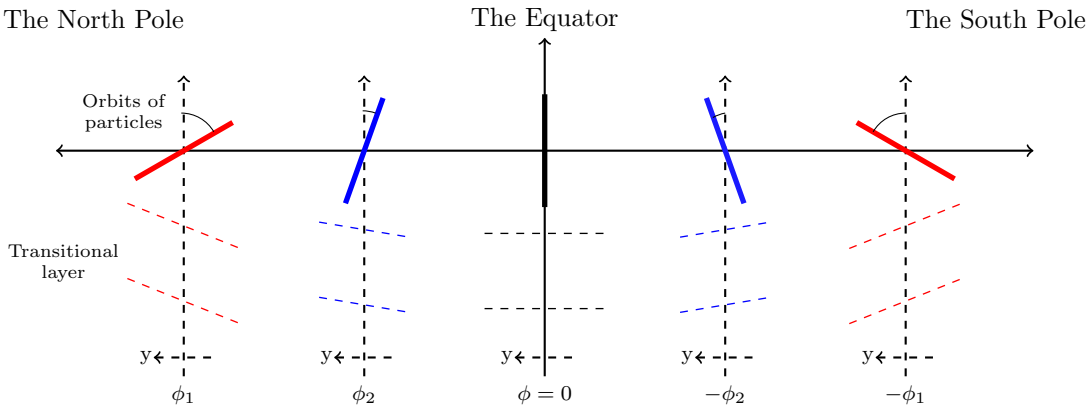


Figure 2: The angle of the inclination of particles' orbits is $\arctan(-d/a)$ [14, 35] and is increasing with the latitude resulting in the three-dimensional profile of the internal water wave [35] (see figure 3). The upper and lower interface of the transitional layer becomes also inclined at the angle ϕ with respect to the local meridional axis. The inclination of the orbits and the interfaces is the result of the Earth's constant rotation.

The uniform flow layer $\mathcal{U}(t)$

In the layer precisely beneath the thermocline particles experience a uniform rectilinear motion expressed physically as a uniform current. The magnitude and direction of the current is equivalent to the wave phase speed c, therefore the velocity field in the uniform flow layer is defined as

$$u = c, \qquad v = w = 0.$$

Following that, the pressure takes the form

$$P(x, y, z, t) = \rho_+ \hat{f} c \left(z - \tilde{f} y \right) + \frac{1}{2} c \rho_+ \hat{f} \left(d_2 + d_1 \right) - \rho_+ g z + P_0.$$

The continuity of all velocity fields and pressures derived above holds across each interface. Moreover, the continuity condition (1) and the kinematic condition (3) are trivially satisfied.

The layer $\mathcal{M}(t)$ above the thermocline

In the layer $\mathcal{M}(t)$ the wave motion is representation of the oscillation of the thermocline. The explicit Pollard-like solution prescribes a periodic zonally travelling wave with a wave speed c and is described in Lagrangian labelling variables [1]. The Lagrangian positions (x, y, z) of fluid particles are functions of labelling variables (q, r, s), where $q \in \mathbb{R}$, $r \in (-r_0, r_0)$ and $s \in (s_0(r), s_+(r))$. We set up the

solution at a fixed latitude ϕ, therefore we take that $r \in (-r_0, r_0)$. Moreover, $s_0(r), s_+(r)$ represent the thermocline and upper boundary of the layer $\mathcal{M}(t)$ for the fixed latitude ϕ, where $s(r) \geq s^* > 0$. We construct the explicit solution for the internal water waves

$$\begin{cases} x = q - be^{-ms}\sin[k(q-ct)], \\ y = r - de^{-ms}\cos[k(q-ct)], \\ z = -d_0 + s - ae^{-ms}\cos[k(q-ct)], \end{cases} \tag{4}$$

where $d_0 > 0$ such that $d_0 < d_1 < d_2$ is introduced to adjust the depth of the thermocline. The solution describes closed circles [14, 35] in a plane slightly tilted to the local vertical (cf. Figure 2), which is caused by the constant rotation of Earth and results in the three-dimensional profile of the wave (cf. Figure 3). For the internal water waves we set the parameter of the amplitude $a > 0$, wave number $k > 0$, whereas the remaining parameters b, d, c, m must be suitably chosen in terms of a, k and the Coriolis parameters $f, \hat{f}$. The wave number $k = 2\pi/L$ corresponds to the wavelength L. Additionally, the upper bound of the amplitude of the internal wave is $1/m$ (see condition (8)) and we propose to call the parameter m as a modified wavenumber (16) — this parameter is also a decay factor of the amplitude of the internal water wave (4). For notational convenience we set

$$\theta = k(q - ct).$$

For the explicit solution in terms of the Lagrangian labelling variables (4) we can easily calculate the velocity and acceleration of the particles

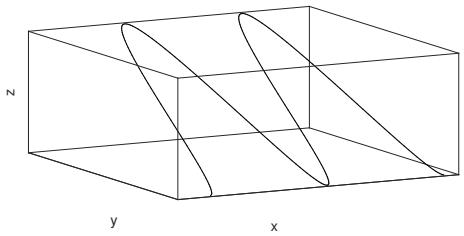


Figure 3: The schematic three-dimensional profile of the internal water waves. The cross-wave tilt is a result of Earth's rotation [14, 35, 38]. At the equator the wave profile is in the vertical plane [3].

$$\begin{cases} u = \frac{Dx}{Dt} = kcbe^{-ms}\cos\theta, \\ v = \frac{Dy}{Dt} = -kcde^{-ms}\sin\theta, \\ w = \frac{Dz}{Dt} = -kcae^{-ms}\sin\theta, \end{cases} \quad \begin{cases} \frac{Du}{Dt} = k^2c^2be^{-ms}\sin\theta, \\ \frac{Dv}{Dt} = k^2c^2de^{-ms}\cos\theta, \\ \frac{Dw}{Dt} = k^2c^2ae^{-ms}\cos\theta, \end{cases}$$

where D/Dt defines the material derivative. The governing equations of the fluid motion above the thermocline are

$$\begin{cases} \frac{Du}{Dt} + \hat{f}w - fv = -\frac{1}{\rho_0}P_x, \\ \frac{Dv}{Dt} + fu = -\frac{1}{\rho_0}P_y, \\ \frac{Dw}{Dt} - \hat{f}u = -\frac{1}{\rho_0}P_z - g. \end{cases} \tag{5}$$

Therefore, checking that (4) is the solution of the governing equations (5) is equivalent to obtaining a compatible pressure. In order to proceed further and to find the pressure we rewrite the governing equations in the Lagrangian labelling variables by using the Jacobian of the mapping (4)

$$\begin{pmatrix} \frac{\partial x}{\partial q} & \frac{\partial y}{\partial q} & \frac{\partial z}{\partial q} \\ \frac{\partial x}{\partial r} & \frac{\partial y}{\partial r} & \frac{\partial z}{\partial r} \\ \frac{\partial x}{\partial s} & \frac{\partial y}{\partial s} & \frac{\partial z}{\partial s} \end{pmatrix} = \begin{pmatrix} 1 - kbe^{-ms}\cos\theta & kde^{-ms}\sin\theta & kae^{-ms}\sin\theta \\ 0 & 1 & 0 \\ mbe^{-ms}\sin\theta & mde^{-ms}\cos\theta & 1 + mae^{-ms}\cos\theta \end{pmatrix}, \tag{6}$$

where the Jacobian determinant is

$$D = 1 + (ma - kb)e^{-ms}\cos\theta - kmabe^{-2ms}.$$

Given the determinant of the Jacobian, the incompressibility condition is satisfied if the determinant is time-independent, thus we take

$$ma - kb = 0. \tag{7}$$

The local diffeomorphic character of the constructed solution is ensured by the inverse function theorem when

$$m^2a^2e^{-2ms^*} < 1, \tag{8}$$

where $s(r) \geq s^* > 0$. From the governing equations (5) we get

$$\begin{aligned} P_x &= -\rho_0 kc[kcb - a\hat{f} + df]e^{-ms}\sin\theta, \\ P_y &= -\rho_0 kc[kcd + bf]e^{-ms}\cos\theta, \\ P_z &= -\rho_0[kc(kca - \hat{f}b)e^{-ms}\cos\theta + g]. \end{aligned}$$

Making use of the Jacobian (6)

$$\begin{pmatrix} P_q \\ P_s \\ P_r \end{pmatrix} = \begin{pmatrix} \frac{\partial x}{\partial q} & \frac{\partial y}{\partial q} & \frac{\partial z}{\partial q} \\ \frac{\partial x}{\partial r} & \frac{\partial y}{\partial r} & \frac{\partial z}{\partial r} \\ \frac{\partial x}{\partial s} & \frac{\partial y}{\partial s} & \frac{\partial z}{\partial s} \end{pmatrix} \cdot \begin{pmatrix} P_x \\ P_y \\ P_z \end{pmatrix},$$

we obtain derivatives with respect to the labelling variables (q, s, r)

$$\begin{aligned}
P_q =& -\rho_0\big[k^3c^2(a^2+d^2-b^2)e^{-ms}\cos\theta + kc(kcb - a\hat{f} + df) + kag\big]e^{-ms}\sin\theta,\\
P_r =& -\rho_0 kc[kcd + bf]e^{-ms}cos\theta,\\
P_s =& -\rho_0\big[k^2c^2m(a^2+d^2-b^2)e^{-2ms}\cos^2\theta - \hat{f}kcmabe^{-2ms} + fkcmbde^{-2ms}\\
&+ k^2c^2b^2me^{-2ms} + (k^2c^2a - kcb\hat{f} + mag)e^{-ms}\cos\theta + g\big].
\end{aligned} \tag{9}$$

Taking into consideration mixed second order derivatives of (9) and the relation (7) we get supplementary relationships between the parameters of the Pollard-like solution

$$kcd + bf = 0, \tag{10}$$

$$mkc^2b + mcdf = k^2c^2a. \tag{11}$$

In the view of the obtained constraints (10), (11) and an arbitrary constant $\tilde{P}_0$ the gradient of the function

$$\begin{aligned}
P(q,r,s,t) =& -\rho_0\bigg[-\frac{1}{2}k^2c^2\left(a^2+d^2-b^2\right)e^{-2ms}\cos^2\theta\\
&-\frac{1}{2}k^2c^2b^2e^{-2ms} + \frac{1}{2}\hat{f}kcabe^{-2ms} - \frac{1}{2}fkcbde^{-2ms}\\
&+\Big(ca\hat{f} - cdf - kc^2b - ag\Big)e^{-ms}\cos\theta + gs\bigg] + \tilde{P}_0,
\end{aligned} \tag{12}$$

is exactly the right-hand side of (9), therefore (12) is the pressure in the layer $\mathcal{M}(t)$ satisfying (5). We require the pressure to be continuous across each interface. Thus evaluating the pressure on the thermocline we define

$$\begin{aligned}
P_0 - \tilde{P}_0 =& \frac{1}{2}\rho_0 kcb(kcb - a\hat{f} + df)e^{-2ms_0} - \Big(\rho_+\hat{f}c - (\rho_+ - \rho_0)g\Big)s_0\\
&+ \rho_+ fcr - \frac{1}{2}c\rho_+\hat{f}(d_2 + d_1) + d_0\rho_+(\hat{f}c - g).
\end{aligned} \tag{13}$$

which is the product of the continuity of the pressure across the thermocline. The solution $s_0(r)$ to the equation (13) represents the thermocline. The upper boundary of the layer $\mathcal{M}(t)$ is specified by setting $s = s_+(r)$ at a fixed value of $r \in (-r_0, r_0)$ with $s_+(r) > s_0(r)$ in (13) so that it also represents an interface. Moreover, the continuity condition of pressure across the thermocline yields

$$\frac{\rho_+ - \rho_0}{\rho_0}(fcd + ag - ca\hat{f}) = kc^2b. \tag{14}$$

and additionally, the pressure must be time-independent hence

$$b^2 = a^2 + d^2. \tag{15}$$

The continuity of the pressure across the thermocline is possible if and only if the conditions (14), (15) and (13) hold for $s = s_0(r)$. From the relations (7), (10) and (11) we get

$$b = \frac{ma}{k}, \qquad d = -\frac{fma}{k^2 c}, \qquad m^2 = \frac{k^4 c^2}{k^2 c^2 - f^2}, \tag{16}$$

respectively. The third equation indicates that $|c| > f/k$. We substitute the above parameters into the equation of continuity of the pressure across the thermocline (14); consequently, we derive the dispersion relation for the nonhydrostatic internal water waves representing the oscillation of the thermocline

$$\left(\frac{\rho_+ - \rho_0}{\rho_0}\right)^2 \left(k^2 c^2 - f^2\right) \left(g - c\hat{f}\right)^2 = c^2 \left(k^2 c^2 + f^2 \frac{\rho_+ - \rho_0}{\rho_0}\right)^2. \tag{17}$$

It is readily seen by comparing the above dispersion relation to the one obtained in [35] that the embodiment of the transitional layer increases the complexity of the dispersion relation. To check the validity of our result we can consider the internal water waves in the equatorial region. For the solution evaluated at the equator the Coriolis parameters are equal to $f = 0$, $\hat{f} = 2\Omega$. Then the dispersion relation (17) becomes

$$\rho_0(kc^2 - 2\Omega c + g) = \rho_+(g - 2\Omega c),$$

which agrees with the dispersion relation obtained in [41] in the absence of currents.

5 Solution for the dispersion relation

The dispersion relation gives the exact value of the wave phase speed for fixed parameters. In our case it is convenient to express the dispersion relation in terms of the non-dimensional variables

$$X = c\sqrt{\frac{k}{\tilde{g}}} \qquad \epsilon = \frac{f}{\sqrt{\tilde{g}k}} \qquad F = \frac{\hat{f}}{f},$$

where $\tilde{g} = g(\rho_+ - \rho_0)/\rho_0 \approx 4 \times 10^{-3}$ is a typical value of the reduced gravity in the equatorial region [32]. The dispersion relation becomes a polynomial equation of degree six $P(X) = 0$, where

$$\begin{aligned} P(X) =& X^6 + \left(2\epsilon^2 \frac{\rho_+ - \rho_0}{\rho_0} - F^2\epsilon^2 \left(\frac{\rho_+ - \rho_0}{\rho_0}\right)^2\right) X^4 + 2\frac{\rho_+ - \rho_0}{\rho_0} F\epsilon X^3 \\ &+ \left(\epsilon^4 \left(\frac{\rho_+ - \rho_0}{\rho_0}\right)^2 + F^2\epsilon^4 \left(\frac{\rho_+ - \rho_0}{\rho_0}\right)^2 - 1\right) X^2 \\ &- 2\frac{\rho_+ - \rho_0}{\rho_0} F\epsilon^3 X + \epsilon^2. \end{aligned} \tag{18}$$

We note that the polynomial obtained in the paper [35] is of degree four. Therefore, the consideration of the series of transitional layers beneath the thermocline increase the degree of the polynomial by two orders.

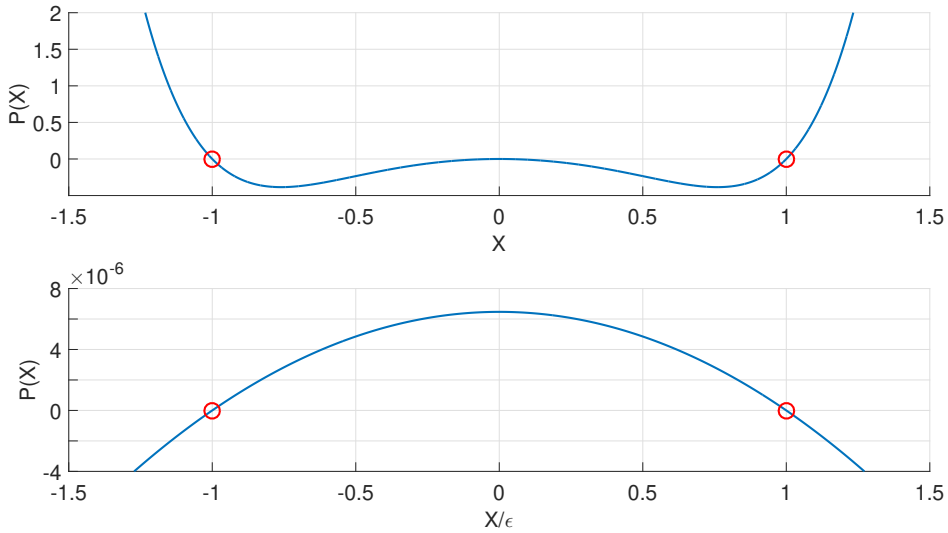


Figure 4: The plot of the polynomial P(X) evaluated at 45° N for $(\rho_+ - \rho_0)/\rho_0 = 4 \times 10^{-3}$, $k = 6.28 \times 10^{-2}\ m^{-1}$. The upper plot shows two roots of order $O(1)$, whereas the lower plot presents two roots of order $O(\epsilon)$.

We seek real roots of (18). Given the real roots of (18), the phase speed of the internal water waves can be found by using the relations introduced in the non-dimensional change of variables. We can readily see that the coefficients of polynomial (18) for a fixed latitude ϕ are the same independently of the hemisphere of Earth. Therefore, we analyse the polynomial for both hemispheres simultaneously. We only exclude the equator from analysis as F is not defined there and the solution particularises there to the Gerstner-like solution for equatorial waves. It is highly complex and complicated to analytically find the exact value of the roots of (18), therefore we focus our attention on estimating the value of the real roots. We consider the internal waves to range from 150 to 250 m [36]. For those wavelengths we obtain $O(F) = 1$, $O(\epsilon) = 10^{-2}$ and we assume $O(\frac{\rho_+ - \rho_0}{\rho_0}) = 10^{-3}$ [32]. Following that, we can estimate the sign of coefficients of the polynomial (18). Hence

$$a_6 = 1, \qquad a_5 = 0, \qquad a_4 > 0, \qquad a_3 > 0, \qquad a_2 < 0, \qquad a_1 < 0, \qquad a_0 > 0,$$

where a_n is the respective coefficient of the term $a_n X^n$ in (18). The polynomial (18) is of degree six, and therefore there are six possible real roots. In order to determine precisely the number of the real roots we use the de Gua corollary to the Fourier-Budan theorem [39].

Corollary. *(de Gua) If in the polynomial $2m+1$ consecutive terms are missing, then if they are between terms of different signs, the polynomial has no less than $2m$ imaginary roots, whereas if the missing terms are between terms of the same sign the polynomial has no less than $2m+2$ imaginary roots.*

As a consequence, the polynomial (18) has at most four real roots. Moreover, evaluating the polynomial for the internal waves at 45° N, $(\rho_+ - \rho_0)/\rho_0 = 4 \times 10^{-3}$ and $k = 6.28 \times 10^{-2}\ m^{-1}$ we can see that indeed the polynomial has four real roots and we can expect two roots of order $O(1)$ and two of order $O(\epsilon)$ (cf. Figure 4). For the polynomial $P(X)$ we infer the estimates

$$
\begin{aligned}
P(\pm 1) &= \pm 2\epsilon F \frac{\rho_+ - \rho_0}{\rho_0} + O(\epsilon^2), \\
P(\pm\epsilon) &= \epsilon^6 \left(1 + 2\frac{\rho_+ - \rho_0}{\rho_0} + \left(\frac{\rho_+ - \rho_0}{\rho_0} \right)^2 \right) > 0, \\
P(1 - \epsilon F) &= 2\epsilon F \left(\frac{\rho_+ - \rho_0}{\rho_0} - 2 \right) + O(\epsilon^2) < 0, \\
P(-1 - \epsilon F) &= 2\epsilon F \left(2 - \frac{\rho_+ - \rho_0}{\rho_0} \right) + O(\epsilon^2) > 0,
\end{aligned}
$$

$$
\begin{aligned}
P(\epsilon + \epsilon^2) &= -2\epsilon^4 + O(\epsilon^6) < 0, \\
P(-\epsilon - \epsilon^2) &= -2\epsilon^4 + O(\epsilon^6) < 0.
\end{aligned}
$$

Following these estimations we can state that there are two roots of order $O(1)$, which belong to the intervals

$$X_1^+ \in (1 - \epsilon F, 1) \qquad X_1^- \in (-1 - \epsilon F, -1), \tag{19}$$

and two roots of order $O(\epsilon)$ in the intervals

$$X_2^+ \in (\epsilon, \epsilon + \epsilon^2) \qquad X_2^- \in (-\epsilon - \epsilon^2, -\epsilon). \tag{20}$$

The non-dimensional change of variables indicates four roots in the dimensional terms. The roots (19) yield a solution close to

$$c \approx \pm\sqrt{\tilde{g}/k},$$

which is a standard internal wave [42] very slightly modified by the rotation of Earth. On the other hand, the roots (20) imply in the dimensional terms second solution approximately

$$c \approx \pm f/k.$$

As a result we can distinguish two modes of waves; one fast mode expressing a standard internal wave altered by the rotation of Earth and second slow with the period close to the inertial period $T_i = 2\pi/f$. It is proposed by Constantin & Monismith [14] to call the slow mode as the inertial Gerstner wave. The slow mode results in waves with a relatively small vertical decay scale — for waves of wavelengths 150 m and 10^4 km the wave speed of the inertial internal Gerstner wave is $c = 2.46 \times 10^{-3}$ m s^{-1} and $c = 16.408$ m s^{-1} with the maximal amplitude $a < 4.212 \times 10^{-7}$ m and $a < 1.9856 \times 10^{-3}$ m, respectively. Nevertheless, the inertial Gerstner waves occur when the transitional layers are introduced, which is in contrast to the results obtained in [35]. In the study of the hydrostatic model [35] there is only one solution of the respective polynomial (only the fast mode equivalent to a standard internal Gerstner wave slightly modified by the rotation of Earth), this is due to the lower order of the polynomial which pertains to the dispersion relation. The inertial Gerstner wave is a nonlinear phenomenon, which in not captured by the linear analysis [14]. Moreover, the study here and in [14] indicate that the slow mode wave is a peculiar marvel that develop in presence of an underlying zonal current.

Acknowledgements

The author is grateful for constructive comments from the referees. The author acknowledges the support of the Science Foundation Ireland (SFI) research grant 13/CDA/2117.

References

[1] A. Bennett. *Lagrangian Fluid Dynamics*. Cambridge Monographs on Mechanics. Cambridge University Press, Cambridge, UK, 2006.

[2] J. P. Boyd. *Dynamics of the Equatorial Ocean*. Springer-Verlag Berlin Heidelberg, Berlin, Germany, 2018.

[3] A. Constantin. On the deep water wave motion. *Journal of Physics A: Mathematical and General*, 34:1405–1417, 2001.

[4] A. Constantin. *Nonlinear Water Waves with Applications to Wave-Current Interactions and Tsunamis*, volume 81. Society for Industrial and Applied Mathematics, Philadelphia, USA, 2011. CBMS-NSF Regional Conference Series in Applied Mathematics.

[5] A. Constantin. On the modelling of equatorial waves. *Geophysical Research Letters*, 39:1–4, 2012.

[6] A. Constantin. Some three-dimensional nonlinear equatorial flows. *Journal of Physical Oceanography*, 43:165–175, 2013.

[7] A. Constantin. Some nonlinear, equatorially trapped, nonhydrostatic internal geophysical waves. *Journal of Physical Oceanography*, 44:781–789, 2014.

[8] A. Constantin and P. Germain. Instability of some equatorially trapped waves. *Journal of Geophysical Research: Oceans*, 118:2802–2810, 2013.

[9] A. Constantin and R. S. Johnson. The dynamics of waves interacting with the Equatorial Undercurrent. *Geophysical & Anstrophysical Fluid Dynamics*, 109:311–358, 2015.

[10] A. Constantin and R. S. Johnson. Current and future prospects for the application of systematic theoretical methods to the study of problems in physical oceanography. *Physics Letters, Section A: General, Atomic and Solid State Physics*, 380:3007–3012, 2016.

[11] A. Constantin and R. S. Johnson. An exact, steady, purely azimuthal equatorial flow with a free surface. *Journal of Physical Oceanography*, 46:1935–1945, 2016.

[12] A. Constantin and R. S. Johnson. An exact, steady, purely azimuthal flow as a model for the Antarctic Circumpolar Current. *Journal of Physical Oceanography*, 46:3585–3594, 2016.

[13] A. Constantin and R. S. Johnson. A nonlinear, three-dimensional model for ocean flows, motivated by some observations of the Pacific Equatorial Undercurrent and thermocline. *Physics of Fluids*, 29:1–21, 2017.

[14] A. Constantin and S. G. Monismith. Gerstner waves in the presence of mean currents and rotation. *Journal of Fluid Mechanics*, 820:511–528, 2017.

[15] B. Cushman-Roisin and J.-M. Becker. *Introduction to Geophysical Fluid Dynamics. Physcial and Numerical Aspects.* Academic Press, Waltham, USA, 2011.

[16] L. Fan, H. Gao, and Q. Xiao. An exact solution for geophysical trapped waves in the presence of an underlying current. *Dynamics of Partial Differential Equations*, 15:201–214, 2018.

[17] I. Gallagher and L. Saint-Raymond. On the influence of the Earth's rotation on Geophysical Flows. In S. Friedlander and D. Serre, editors, *Handbook of Mathematical Fluid Dynamics*, volume 4, pages 201–329. North-Holland, 2007.

[18] T. Garrison and R. Ellis. *Oceanography: An Invitation to Marine Science*. Cengage Learning, Boston, USA, 2014.

[19] A. E. Gill. *Atmosphere-Ocean Dynamics*. Academic Press, San Diego, USA, 1982.

[20] D. Henry. An exact solution for equatorial geophysical water waves with an underlying current. *European Journal of Mechanics, B/Fluids*, 38:18–21, 2013.

[21] D. Henry. Internal equatorial water waves in the f-plane. *Journal of Nonlinear Mathematical Physics*, 22:499–506, 2015.

[22] D. Henry. Equatorially trapped nonlinear water waves in a β-plane approximation with centripetal forces. *Journal of Fluid Mechanics*, 804:1–11, 2016.

[23] D. Henry. Exact equatorial water waves in the f-plane. *Nonlinear Analysis: Real World Applications*, 28:284–289, 2016.

[24] D. Henry. On three-dimensional Gerstner-like equatorial water waves. *Phylosophical Transactions of the Royal Society of London A: Mathematical, Physical and Engineering Sciences*, 376:1–16, 2017.

[25] H.-C. Hsu. An exact solution for nonlinear internal equatorial waves in the f-plane approximation. *Journal of Mathematical Fluid Mechanics*, 16:463–471, 2014.

[26] H.-C. Hsu. An exact solution for equatorial waves. *Monatshefte für Mathematik*, 176:143–152, 2015.

[27] D. Ionescu-Kruse. On Pollard's wave solution at the equator. *Journal of Nonlinear Mathematical Physics*, 22:523–530, 2015.

[28] D. Ionescu-Kruse. Instability of Pollard's exact solution for geophysical ocean flows. *Physics of Fluids*, 28:1–10, 2016.

[29] D. Ionescu-Kruse. On the short-wavelength stabilities of some geophysical flows. *Phylosophical Transactions of the Royal Society of London A: Mathematical, Physical and Engineering Sciences*, 376:1–21, 2017.

[30] D. Ionescu-Kruse. A three-dimensional autonomous nonlinear dynamical system modelling equatorial ocean flows. *Journal of Differential Equations*, 264(7):4650–4668, 2018.

[31] R. S. Johnson. Application of the ideas and techniques of classical fluid mechanics to some problems in physical oceanography. *Phylosophical Transactions of the Royal Society of London A: Mathematical, Physical and Engineering Sciences*, 376:1–19, 2017.

[32] W. S. Kessler and M. J. McPhaden. Oceanic equatorial waves and the 1991-93 El Niño. *Journal of Climate*, 8:1757–1774, 1995.

[33] M. Kluczek. Exact and explicit internal equatorial water waves with underlying currents. *Journal of Mathematical Fluid Mechanics*, 19:305–314, 2017.

[34] M. Kluczek. Equatorial water waves with underlying currents in the f-plane approximation. *Applicable Analysis*, 97:1867–1880, 2018.

[35] M. Kluczek. Exact Pollard-like internal water waves. *Journal of Nonlinear Mathematical Physics*, 26:133–146, 2019.

[36] J. N. Moum, J. D. Nash, and W. D. Smyth. Narrowband oscillations in the upper equatorial ocean. Part I: Interpretation as shear instabilities. *Journal of Physical Oceanography*, 41:397–411, 2011.

[37] J. Pedlosky. *Geophysical Fluid Dynamics*. Springer-Verlag Berlin Heidelberg, Virginia, USA, 1987.

[38] R. T. Pollard. Surface waves with rotation: An exact solution. *Journal of Geophysical Research*, 75:15–32, 1970.

[39] V. V. Prasolov. *Polynomials*. Springer-Verlag Berlin Heidelberg, Berlin, Germany, 2004.

[40] A. Rodríguez-Sanjurjo. Global diffeomorphism of the Lagrangian flow-map for Pollard-like solutions. *Annali di Matematica Pura ed Applicata (1923–)*, 197:1787–1797, 2018.

[41] A. Rodríguez-Sanjurjo. Internal equatorial water waves and wave–current interactions in the f-plane. *Monatshefte für Mathematik*, 186:685–701, 2018.

[42] R. Stuhlmeier. Internal Gerstner waves: Applications to dead water. *Applicable Analysis*, 93:1451–1457, 2014.

[43] G. K. Vallis. *Atmospheric and Oceanic Fluid Dynamics: Fundamentals and Large-Scale Circulation*. Cambridge University Press, New York, USA, 2006.

[44] F. J. von Gerstner. Theorie der Wellen samt einer daraus abgeleiteten Theorie der Deichprofile. *Annalen der Physik*, 32:412–445, 1809.